Rate-type creep law of aging concrete based on Maxwell chain

Z.P. BAŽANT (1), S.T. WU (2)

It is shown that the linear creep law of concrete can be characterized, with any desired accuracy, by a rate-type creep law that can be interpreted by a Maxwell chain model of time-variable viscosities and spring moduli. Identification of these parameters from the test data is accomplished by expanding into Dirichlet series the relaxation curves, which in turn are computed from the measured creep curves. The identification has a unique solution if a certain smoothing condition is imposed upon the relaxation spectra. The formulation is useful for the step-by-step time integration of larger finite element systems because it makes the storage of stress history unnecessary. For this purpose a new, unconditionally stable numerical algorithm is presented, allowing an arbitrary increase of the time step as the creep rate decays. The rate-type formulation permits establishing a correlation with the rate processes in the microstructure and thus opens the way toward rational generalizations to variable temperature and water content. The previously developed Kelvin-type chain also permits such a correlation, but its identification from test data is more complicated.

BASIC NOTATIONS

$E(t) = E_R(t,t) = 1/J(t,t)$ = instantaneous Young's modulus of concrete;

E'' = pseudo-instantaneous Young's modulus in Eq. (18);

$E_R(t, t')$ = relaxation modulus = stress in time t caused by a constant unit strain enforced in time t' (Eq. (1));

$\tilde{E}_R$ = given data on E_R;

E_μ = modulus of μth spring in Maxwell chain, fig. 1, Eq. (3);

E_∞ = ultimate relaxation modulus (fig. 1, Eq. (6));

$E_{t\mu}$ = coefficients of smoothing expressions (9), (10), (11);

$J(t, t')$ = creep function (or compliance) = stress at time t caused by a constant unit stress acting since time t' (Eq. 1);

n, m = number of units in Maxwell chain, $m = n - 1$;

t, t' = time from casting of concrete (in days);

t', t_0 = time of application of constant stress or strain;

w_1, w_2, w_3 = weights in the penalty term in Eq. (8);

ε, σ = strain and stress;

$\varepsilon^0, \varepsilon''$ = prescribed stress-independent inelastic strain (Eq. (1)) and pseudo-inelastic strain in Eq. (18);

(1) Professor of Civil Engineering, Northwestern University, Evanston, Ill. 60201, Active Member RILEM.

(2) Graduate Research Assistant, Northwestern University (presently Staff Engineer, Sargent and Lundy, Engineers, Chicago, Ill.).

σ_μ = hidden stresses in Eq. (3) = stress in the μth spring in Maxwell chain (fig. 1, Eq. (3));

η_μ = viscosity of the μth dashpot Maxwell chain (fig. 1, Eq. (3));

λ_μ = parameter given by Eq. (16);

$\tau_\mu = \eta_\mu/E_\mu$ = relaxation time of the μth unit in Maxwell chain (fig. 1).

Subscripts : r, s — for discrete times t_r, t_s in step-by-step analysis;

α, β for selected values of t' and $(t - t')$ used in the least square condition;

μ — for the μth unit in Maxwell chain (fig. 1).

Dot stands for time derivative; $\dot{\varepsilon} = d\varepsilon/dt$, e.g.

INTRODUCTION

A rate-type creep law, i.e. a stress-strain relation in form of a differential equation, has two important advantages over the integral-type creep law involving hereditary integrals. First, whereas the integral-type law requires storing the complete history of stress or strain in the structure (which overtaxes, in the case of larger finite element systems, the capacity of rapid access memory of even the largest computers), the rate-type law necessitates only the current values of stresses, strains, and a few hidden state variables to be stored. Second, the rate-type law may be brought in correlation with the rate processes in the microstructure, associating the hidden (or internal) state variables with some sort of microstrains or microstresses. This allows the dependence of various material parameters upon temperature and water content to be predicted to some degree from a mathematical theory of the creep mechanism [3], reducing thus considerably the degree of arbitrariness in the identification of material parameters from experimental data.

Recently [6] it has been shown that the stress-strain law of concrete viewed as a linear time-variable viscoelastic material can be approximated, with any desired accuracy, by a rate-type creep law based on the Kelvin chain model with age-dependent properties. This approximation has enabled formulation of a very efficient new algorithm of step-by-step time integration of creep problems [6]. Unfortunately, however, the Kelvin chain has some disadvantages. The Kelvin-type formulations with such relations between age-dependent viscosities and spring moduli for which the identification of material parameters from the test data is simple, either yield negative spring moduli for some periods of time or lead to non-standard relations for the dashpots [3], either of which precludes the correlation with the rate processes in the microstructure, mentioned before. Only one Kelvin-type formulation, namely that with proportionate age-dependence of viscosities and spring moduli, is free from both drawbacks [3]. But it is more complicated and the identification of its parameters from test data is more involved.

In classical viscoelasticity it is proved that any material can be described with any desired accuracy either by a Kelvin chain or by a Maxwell chain. These chains are, therefore, mutually equivalent [22] (and also equivalent to any other possible model). It is natural to anticipate this property to hold also in the case of aging. Thus, in view of the drawbacks of the Kelvin chain, attention is focused in this study on the Maxwell chain, despite the fact that its relationship to the creep tests may be conceptually less convenient.

CREEP LAW OF A LINEAR AGING MATERIALS

If stresses remain less than about 0.4 of the strength and no strain reversals occur, the creep law of concrete may be assumed as linear [19, 3]. In the integral-type formulation, the uniaxial creep law may be introduced in either of the following two equivalent forms [3] :

$$\varepsilon(t) - \varepsilon^0(t) = \int_0^t J(t, t')\, d\sigma(t'), \quad \sigma(t) \int_0^t E_R(t, t')\,[d\varepsilon(t') - d\varepsilon^0(t')] \qquad (1)$$

where the integrals are Stieltjes integrals, t = time from casting of concrete; σ = stress; ε = strain; $\varepsilon^0(t)$ = given stress-independent inelastic strain; $J(t, t')$ = creep function (called also creep compliance) = strain at time t caused by a constant unit stress acting since time t'; $E_R(t, t')$ = relaxation function (called also relaxation modulus) = stress at time t caused by a constant unit strain introduced at time t'; $1/J(t, t) = E_R(t, t) = E(t)$ = instantaneous Young's modulus (usually taken as $1/J$ for $t - t' \simeq 1$ mn). The relation between functions J and E_R may be obtained by considering the strain history to be a unit step function, that is, $\varepsilon = 1$ for $t \geqslant t_0$ and $\varepsilon = 0$ for $t < t_0$, $\varepsilon^0 = 0$, in which case the response is, by definition, $\sigma(t) = E_R(t, t_0)$ for $t \geqslant t_0$. Substitution into the first of Eq. (1) yields the Volterra's integral equation :

$$J(t, t_0)\, E(t_0) + \int_{t_0}^{0} J(t, t') \frac{\partial E_R(t', t_0)}{\partial t'}\, dt' = 1 \qquad (2)$$

The rate-type formulation may be based on the Maxwell chain model (fig. 1), which gives the stress-strain relations :

$$\sigma = \sum_\mu \sigma_\mu, \quad \dot{\varepsilon} - \dot{\varepsilon}^0 = \sigma_\mu/E_\mu + \sigma_\mu/\eta_\mu \quad (\mu = 1, 2, \ldots, n) \qquad (3)$$

where σ_μ are the hidden stresses (or partial stresses) in the individual Maxwell units of the chain.

EXPANSION OF RELAXATION FUNCTION IN DIRICHLET SERIES

Similarly as in the case of Kelvin-type chains [5], a unique characterization of the model requires some relationship between $\eta_\mu(t)$ and $E_\mu(t)$ to be assumed. The simplest assumption is :

$$\tau_\mu = \eta_\mu/E_\mu = \text{const.} \quad (\mu = 1, 2, \ldots n) \qquad (4)$$

(This ratio is called relaxation time.) Then, considering again the strain history as a step function, $\varepsilon = 1$ for $t \geq t'$ and $\varepsilon = 0$ for $t < t'$ ($\varepsilon^0 = 0$), the integral of the second Eq. (3) for the initial condition $\sigma_\mu(t') = E_\mu(t')$ is

$$\sigma_\mu(t) = E_\mu(t')\, e^{-(t-t')/\tau_\mu} \tag{5}$$

Comparison of the expression for $\sigma = \sum_\mu \sigma_\mu$ with (1) shows that

$$E_R(t, t') = \sum_{\mu=1}^{m} E_\mu(t')\, e^{-(t-t')/\tau_\mu} + E_\infty(t') \tag{6}$$

where $m = n - 1$; $E_\infty(t')$ is written here under the assumption that for $\mu = n$ there is $\eta_\mu \to \infty$ or $\tau_\mu \to \infty$, i.e., the last spring in figure 1 is not coupled to any dashpot.

Eq. (6) represents an expansion of the relaxation function into the series of real exponentials, called Dirichlet series [14]. Fitting of curves by this series is a difficult mathematical problem because $E_\mu(t')$ are unstable functions of E_R [17]. The problem is generally not tractable unless the τ_μ — s are suitably selected and certain smoothing conditions are applied. After much computing experience, the procedure outlined below has been found to work satisfactorily.

To obtain the Maxwell chain model fitting given relaxation data, one can select a number of t'-values (i.e., $t' = t'_\alpha$, $\alpha = 1, 2, 3, \ldots$; see figure 9 below) and expand $E_R(t, t')$ as a function of t alone for each fixed t'_α separately, according to Eq. (6). As has been mentioned, the τ_μ-values must be chosen in advance. With a sufficiently close distribution of τ_μ-values the relaxation curves can be fitted with any desired accuracy (provided the slope of the curve in $\log(t - t')$-scale is nowhere too large). For uniqueness of fit, however, the τ_μ-s may not be too close to each other (unless w_1, w_2, w_3 in Eq. (8) below are chosen very large). A pratically suitable choice is

$$\tau_\mu = 10^{\mu-1}\, \tau_1 \quad (\mu = 1, \ldots, m) \tag{7}$$

Here τ_1 should roughly coincide with the point where the relaxation curve begins to descend, and τ_m with the longest $(t - t')$ considered. (In comparison with the usual experimental error it even suffices to use $\tau_\mu = 60^{\mu-1}\, \tau_1$, which leads to about 1.5 times fewer τ_μ-s and σ_μ-s for the same time range to be covered (*cf.* fig. 19 below). The best method of fitting was found to be the method of least squares based on minimizing the expression

$$\Phi = \sum_\beta [E_R(t_\beta, t') - \tilde{E}_R(t_\beta, t')]^2 + w_1 \sum_{\mu=1}^{m-1} (E_{\mu+1} - E_\mu)^2 + w_2 \sum_{\mu=1}^{m-2} (E_{\mu+2} - 2\,E_{\mu+1} + E_\mu)^2 + w_3 \sum_{\mu=1}^{m-3} (E_{\mu+3} - 3\,E_{\mu+2} + 3\,E_{\mu+1} - E_\mu)^2 \tag{8}$$

Here $\tilde{E}_R$ denotes the given values of the relaxation function to be fitted, E_R stands for expression (6). The second sum represents a penalty term which is added as a smoothing device [6], intended to minimize the first, second and third differences between E_1, E_2, E_3, ..., and also to reduce the sensitivity of E_μ to the scatter of data. Suitable values for w_1, w_2, w_3 can be assessed only by computing experience (see Table I below). They should not be larger than necessary. (For very smooth data one can put $w_1 = w_2 = w_3 = 0$.) Subscript β stands for a series of $(t - t')$-values, $(t - t')_\beta$, $\beta = 1, 2, \ldots$, which are best chosen as uniformly distributed in log $(t - t')$-scale, four values per decade (see fig. 9 below); $t_\beta - t' = (t - t')_\beta = 10^{\frac{1}{4}}(t - t')_{\beta-1}$.

The minimizing conditions are $\partial\Phi/\partial E_\mu = 0$, ($\mu = 1, 2, \ldots, m$) and $\partial\Phi/\partial E_\infty = 0$, which yields a system of $(m + 1)$ linear algebraic equations for E_μ and E_∞.

Because the slope of relaxation curve is everywhere non-positive, all E_μ-s are non-negative.

Other types of Maxwell chain representation could be obtained if Eq. (4) is replaced by other relations between η_μ and E_μ, including their derivatives. But the above representation is certainly the simplest one, and because it allows fitting the creep curves with any desired accuracy, there is no need for examining other representations. (Such a need could possibly arise when creep at variable environment is considered. But the success in fitting the data at variable temperature in Ref. [7] suggests that this is probably not the case.)

The computed values of E_μ as functions of log t' usually exhibit too much scatter (as is seen from fig. 11-17 and from the dependence of relaxation curves on t' in fig. 9, all discussed in the sequel. Smoothing with respect to age was therefore deemed to be appropriate. The expressions (t' in days) :

$$E_\mu(t') = E_{0_\mu} + \sum_{i=1}^{3} E_{i_\mu}/[1 + t'/(3 \times 30^{i-1})] \tag{9}$$

$$E_\mu(t') = E_{0_\mu} + \sum_{i=1}^{3} E_{i_\mu}\, [\log (1 + t')]^i \tag{10}$$

were found best suited for this purpose (for 1 day $\leq t' \leq$ 10,000 days). Expression of the type (t' in days) :

$$E_\mu(t') = E_{0_\mu} + E_{1_\mu}\, t'^{1/8} + E_{2_\mu}\, t'^{1/4} + E_{3_\mu}\, t'^{1/2} + E_{4_\mu}\, t'^{3/4} \tag{11}$$

(and also with other exponents) gives good fits, too, but usually not as close as Eq. (9) or (10). Hovewer, Eq. (11) seems to be best for extrapolation into very high ages t'. The constants E_{0_μ}, ..., E_{3_μ} are easily determined by the method of least squares. (Their values for various data are presented in Table I below, along with suitable values found for the coefficients w_1 and w_2 of the penalty term in Eq. (8)).

A smooth change of E_μ with μ has been achieved by means of the weights w_1, w_2, and w_3 in Eq. (8), as has already been mentioned. (With $w_1 = w_2 = 0$ the scatter of E_μ was sometimes so large that some of the E_μ-values were even negative.) Changes in w_1 and w_2 can occasionally change E_μ-values by as much as 10 %, while the fit of the original creep data (fig. 2, 3 below) still remains quite good. This is, of course, within the range of dispersion of the original data but indicates that for scattered data the solution of the fitting problem exhibits no strong uniqueness (even if τ_μ-s are selected properly.) For the data in which J had to be extrapolated into large t', different extrapolation curves have been examined to obtain the smoothest possible $E_\mu(t')$.

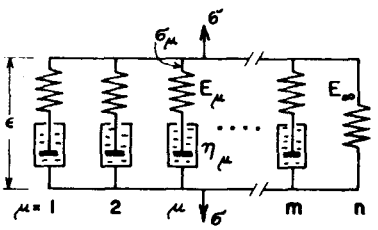

Fig. 1

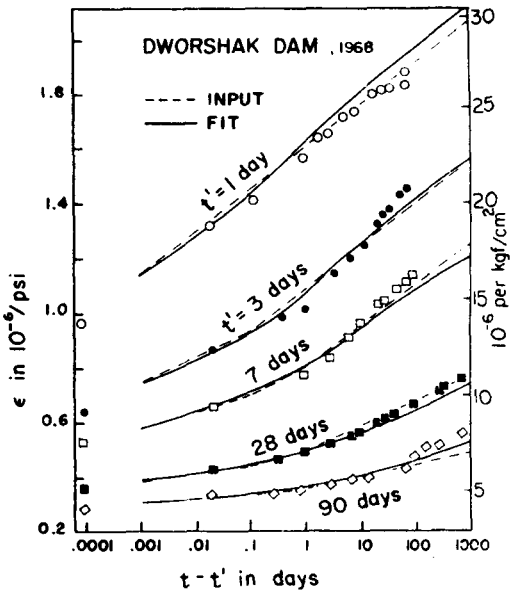

Fig. 2.

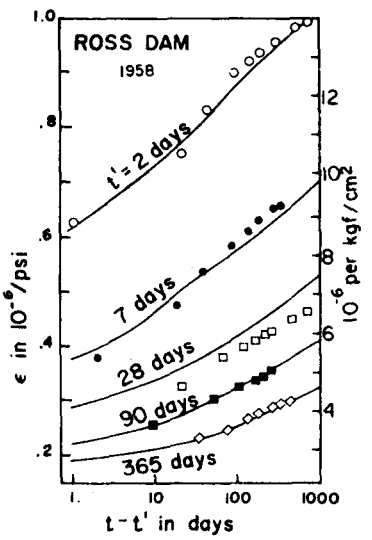

Fig. 3.

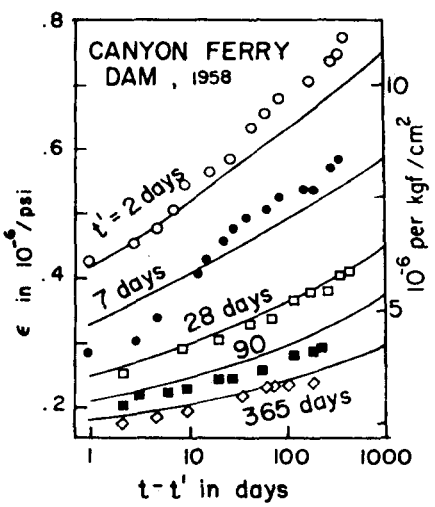

Fig. 4.

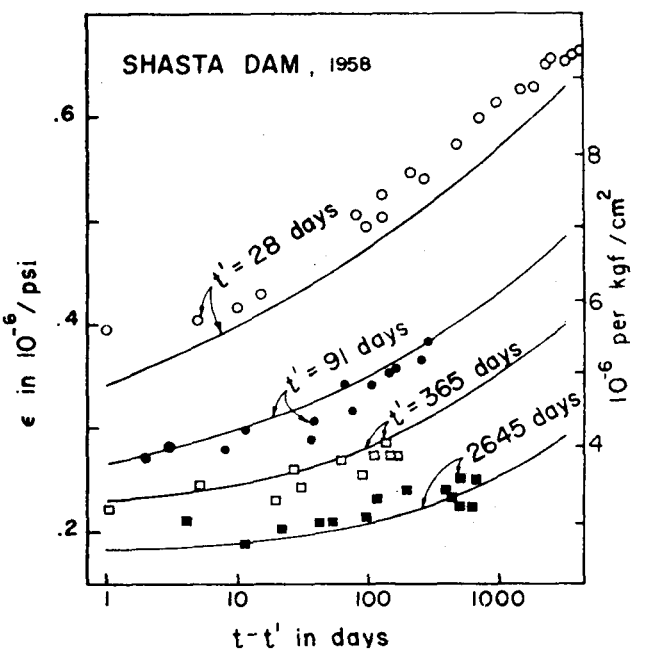

Fig. 5.

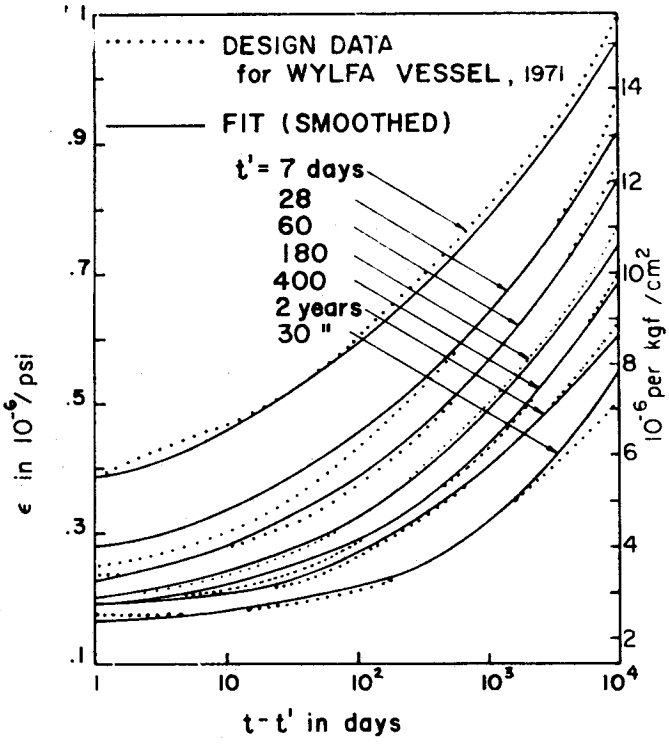

Fig. 6.

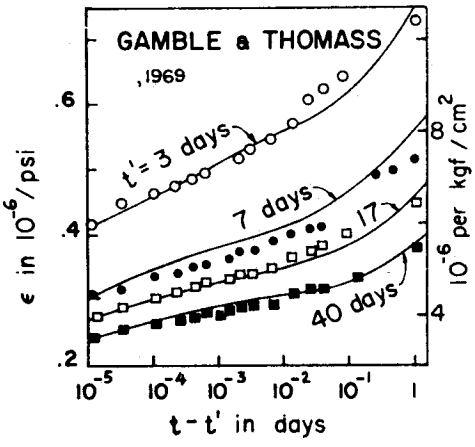

Fig. 7.

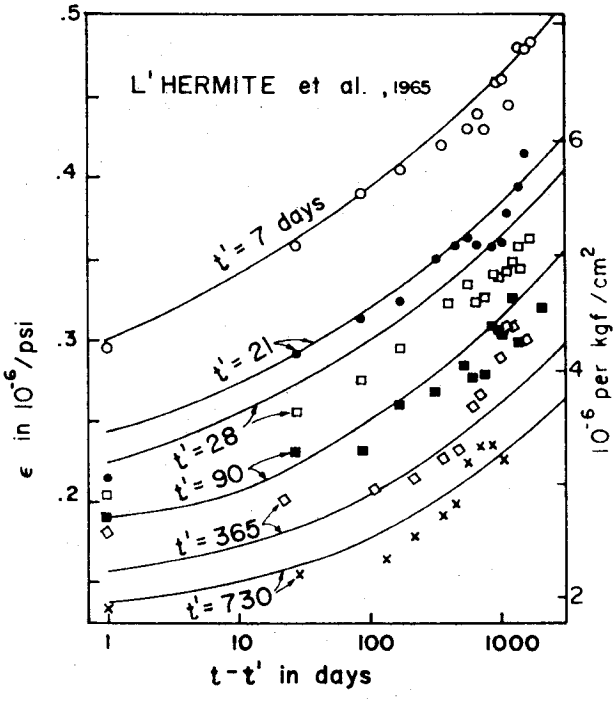

Fig. 8.

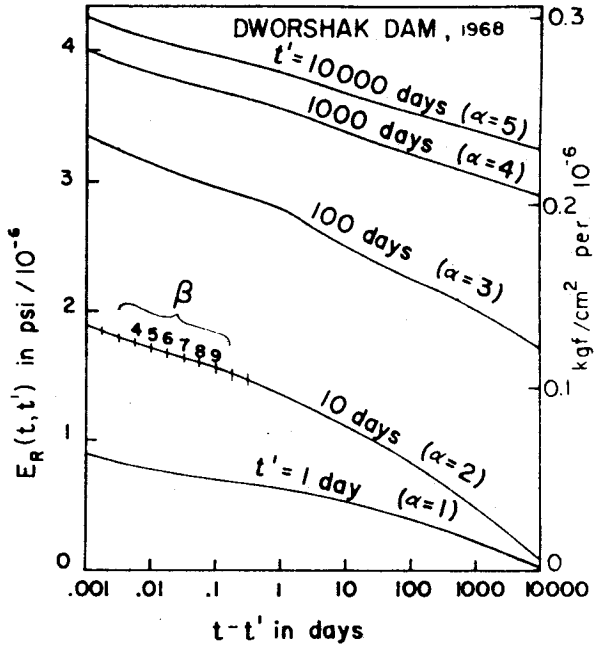

Fig. 9.

TABLE I

Figure	2, 10, 11, 18	3, 9, 12	4, 13	5, 14	6, 15	7, 16	8, 17
Reference	[14]	[15] [16]	[15] [17] [16]	[15] [16]	[18]	[19]	[20]
Temperature	70°F	~ 70°F	~ 70°F	~ 70°F	68°F	75°F	-
Humidity	sealed	sealed	sealed	sealed	sealed	94%	in water
28-day cyl. strength (psi)	2080	4970	2920	3230	6600	4900	~ 5600
Stress-strength ratio	.21 to .385	≤ .33	≤ .33	≤ .33	≤ .36	.42 to .46	0.25
Water-cement ratio	.56	.56	.50	.58	.42	.70?	.49
Aggr.-cement ratio	6.8	-	-	-	4.4	5.1	-
Size of cylinder (inch)	6 x 18	6 x 16	6 x 16	6 x 26	6 x 12	4 x 10 & other	-
Type of cement	II	II	II	IV	II	I	-
Type of aggr.	granite -gneiss	-	-	-	foramiferal limestone	crushed greywacke	-
Max. aggr. size (inch)	1.5	1.5	1.5	1.5	1.5	.19	-

CONVERSION OF CREEP DATA INTO RELAXATION DATA

The least square procedure described above permits direct determination of Maxwell chain parameters E_μ and η_μ from stress relaxation data.

Although several relaxation data have been published in the literature [11, 23, 12, 8, 16, 26, 24, 15], none of them suffice for determination of $E_R(t, t)$. The range of elapsed times measured was sufficient in the tests of Rostásy *et al.* [24], and companion creep tests were also made, but only a single age at loading, t', was used. In such a case the fitting problem has no unique solution (1).

Therefore, one must resort to creep test data, converting them to relaxation data. This conversion has been discussed in detail elsewhere [1], and only a brief description will be given here. Relaxation function $E_R(t, t')$ must be solved from the Volterra's equation (2). This is best accomplished numerically, subdividing time t by discrete times $t_1, \ldots, t_N$ into N time steps $\Delta t_r = t_r - t_{r-1} (r = 2, 3, \ldots, N)$. It is convenient to put $t_0 = t_1$, expressing the fact that in creep tests with $\sigma =$ constant the first strain increment in time t_0 is instantaneous, i.e., $\Delta t_1 = 0$. If the trapezoidal rule is used to approximate the integral in Eq. (2) and the forms of Eq. (2) for $t = t_r$ and $t = t_{r-1}$ are subtracted, the following recurrent equation (whose error order is Δt^2) is obtained [2] :

$$\Delta E_{R_r} = -(J_{r,r} + J_{r,r-1})^{-1} \sum_{s=1}^{r-1} \Delta E_{R_s} (J_{r,s} + J_{r,s-1} - J_{r-1,s} - J_{r-1,s-1}) \quad (r = 2, 3, 4, \ldots, N) \quad (12)$$

where $\Delta E_{R_r} = E_R(t_r, t_0) - E_R(t_{r-1}, t_0)$, $J_{r,s} = J(t_r, t_s)$, and $\Delta E_{R_1} = E(t_0) =$ starting value. The time step Δt_r is best chosen as increasing in a constant ratio. With regard to the scatter of creep data, the subdivision $(t_r - t_0) = 10^{\frac{1}{4}}(t_{r-1} - t_0)$, (i.e., 4 equal steps per decade in log $(t - t_0)$-scale) was found to give sufficient accuracy. At the same time, times t_r chosen in this manner are suitable for use as times t_β in the least square condition (8).

The first time step Δt_2 should be chosen smaller than the value of the elapsed time $t - t_0$ for which the creep curve begins to rise significantly (and also smaller than τ_1, the shortest retardation time).

For conversion of the creep function into the relaxation function it is necessary to know $J(t, t')$ for any

(1) Assume that only the data on $J(t, t_0)$ and $E_R(t, t_0)$ for a single t_0 — value are available. $J_{3,2}$ can be computed from Eq. (12) for $r = 3$. But then one needs to choose some value for $J_{4,2}$ to be able to compute $J_{4,3}$ from Eq. (12) for $r = 4$. For $r = 5$ one must choose $J_{5,2}$ and $J_{5,3}$ to compute $J_{5,4}$, etc. Thus, it is always possible to find such $J(t, t')$ that matches a given single creep curve and a single relaxation curve exactly. In fact, infinitely many such $J(t, t')$ exist. Consequently, the attempts [24, 16, 12] to demonstrate the validity of the superposition principle on the basis of such incomplete data are of little value. They would be conclusive only if aging were absent or its effect were known in advance.

values of t' and $t - t'$ within the time range considered. When the information on $J(t, t')$ consists of a set of measured values, interpolation must be used. For this purpose a FORTRAN IV subroutine (listed for another purpose in Ref. [1], has been written. It uses as input a two-dimensional array of J-values for selected discrete values of t' and $(t - t')$ and assumes that between them the function $J(t, t')$ varies linearly with $\log t'$, as well as with $\log(t - t')$. Since this assumption is close to reality even for large time intervals, relatively few values of $J(t, t')$ are needed as input. In view of the large scatter of data on concrete, the input values have been determined by smoothing visually the measured curves of $J(t, t')$ versus $\log(t - t')$ for various fixed t'. Because no creep data are known whose range of t' would match the range of $(t - t')$, an extrapolation into high values of t' has been necessary. It has been carried out in the plots of $J(t, t')$ versus $\log(t - t')$ by hand, assuming a similar trend with t' as in the few known tests of old concrete [11, 13]. This, of course, has introduced some degree of arbitrariness into the fitting problem.

ALGORITHM OF STEP-BY-STEP INTEGRATION OF CREEP PROBLEMS

If the usual step-by-step integration methods, such as the Euler method, Runge-Kutta methods or predictor-corrector methods, are applied to Eq. (3), the time step cannot exceed the shortest relaxation time since otherwise numerical instability would occur. Such a restriction is practically unacceptable and a different algorithm must be developed.

Let time t be subdivided by discrete times t_0, t_1, t_2, ... into time steps $\Delta t_r = t_r - t_{r-1} (r = 1, 2, \ldots)$. One can verify by back substitution that the integral of the second Eq. (3) satisfying the initial condition $\sigma_\mu = \sigma_{\mu r-1}$ at $t = t_{r-1}$ is

$$\sigma_\mu(t) = e^{-f_\mu(t)} \left\{ \sigma_{\mu r-1} + \int_{t_{r-1}}^{t} e^{f_\mu(t')} E_\mu(t') [d\varepsilon(t') - d\varepsilon^0(t')] \right\} \quad (13)$$

where

$$f_\mu(t) = \int_{t_{r-1}}^{t} [E_\mu(t')/\eta_\mu(t')]\, dt' \quad (13\,a)$$

For small time steps one may assume that $d\varepsilon/dt$, $d\varepsilon^0/dt$ and E_μ are constant within each time step Δt_r and vary discontinuously at times t_r. Furthermore, using relation (4), $E_\mu(t) = (t - t_{r-1})/\tau_\mu$. Putting $t = t_r$, Eq. (13) then becomes

$$\sigma_{\mu r} = \sigma_{\mu r-1} e^{-\Delta t_r/\tau_\mu} - e^{-\Delta t_r/\tau_\mu} E_{\mu r-\frac{1}{2}} \frac{\Delta\varepsilon_r - \Delta\varepsilon_r^0}{\Delta t_r} \int_{t_{r-1}}^{t_r} e^{(t' - t_{r-1})/\tau_\mu}\, dt' \quad (14)$$

or

$$\sigma_{\mu r} = \sigma_{\mu r-1} e^{-\Delta t_r/\tau_\mu} + \lambda_{\mu r} E_{\mu r-\frac{1}{2}} (\Delta\varepsilon_r - \Delta\varepsilon_r^0) \quad (\mu = 1, 2, \ldots, n) \quad (15)$$

where

$$\lambda_{\mu r} = (1 - e^{-\Delta t_r/\tau_\mu})\, \tau_\mu/\Delta t_r \quad (16)$$

Here subscript r stands for time t_r, e.g., $\sigma_{\mu r} = \sigma_\mu(t_r)$; and subscript $s - \frac{1}{2}$ refers to the average value in the time step, i.e., $E_{\mu r-\frac{1}{2}} = \frac{1}{2}\{E_{\mu r-1} + E_{\mu r}\}$.

In Eq. (15) one has gained a recurrent formula for $\sigma_{\mu r}$. According to Eq. (3), $\Delta\sigma_r = \sum_\mu \Delta\sigma_{\mu r}$. This yields

$$\Delta\varepsilon_r = \Delta\sigma_r/E_r'' + \Delta\varepsilon_r'' \quad (17)$$

where

$$E_r'' = \sum_{\mu=1}^{m} \lambda_{\mu r} E_{\mu r-\frac{1}{2}} + E_{\infty r-\frac{1}{2}} \quad (18)$$

$$E_r'' \Delta\varepsilon_r'' = \sum_{\mu=1}^{m} \{1 - e^{-\Delta t_r/\tau_\mu}\} \sigma_{\mu r-1} + E_r'' \Delta\varepsilon_r^0 \quad (19)$$

For generalizations to variable temperature [7] it is noteworthy that Eq. (15)-(19) also apply when $\eta_\mu/E_\mu \neq$ constant, provided that τ_μ is replaced by $\tau_{\mu r-\frac{1}{2}} = (\eta_\mu/E_\mu)_{r-\frac{1}{2}}$. This follows from Eq. (13 a) assuming that η_μ/E_μ is constant within each time step.

If in a given creep problem the stresses have already been computed up to the time t_{r-1}, the values E_r'' and $\Delta\varepsilon_r''$ may be determined from Eq. (18) and (19). Eq. (17) may then be regarded as a fictitious linear elastic stress-strain law, in which $\Delta\varepsilon_r'' =$ pseudo-inelastic strain increment and $E_r'' =$ pseudo-instantaneous elastic modulus. Thus, creep structural analysis may proceed in each time step Δt_r as follows: 1) Compute $\lambda_{\mu r}$, E_r'', and $\Delta\varepsilon_r''$ for every point or finite element of the structure, using the stress values for t_{r-1}. 2) Solving the elastic structure with moduli E_r'', compute $\Delta\sigma_r$ and σ_r caused by $\Delta\varepsilon''$ (and the change of loads or boundary displacements during Δt_r) for every point or element. 3) Compute $\sigma_{\mu r}$ ($\mu = 1, 2, \ldots, n$) for every point or element from Eq. (15), discard the values of σ_{r-1} and $\sigma_{\mu r-1}$ and go to the next step Δt_{r+1}.

The above algorithm can be easily generalized to the case of multiaxial stress, writing analogous equations in terms of volumetric and deviatoric stress and strain components.

To examine briefly whether the algorithm is prone to numerical instability, attention may be restricted to the solution of stress produced by a prescribed strain history. Eq. (15) may then be viewed as a nonhomogeneous linear difference equation for the discrete variable $\sigma_{\mu r}$ ($r = 1, 2, 3, \ldots$). The homogeneous part of Eq. (15), arising by deletion of the term with $\Delta\varepsilon_r$, has the solution of form $\sigma_{\mu r} = a^r$ whose insertion in Eq. (16) yields the characteristic equation $a = e^{-\Delta t_r/\tau_\mu}$. Since $0 < a < 1$, the solutions of the homogeneous part of Eq. (15) are of an exponentially decaying character and no numerical instability (unbounded magnification of numerical error) can occur. The nonhomogeneous equation (17) must then be numerically stable, too, and noting that $\sigma_r = \sum \sigma_{\mu r}$ it is seen that the same applies for σ_r. (Excellent stability and accuracy of the algorithm has been confirmed by computation of the fits in figures 2 and 3 below, with time steps increasing in a geometric progression, i.e. constant in a logarithmic time scale.) (It is noteworthy that, on the other hand, the step-forward difference approximations of Eq. (3) are numerically unstable when Δt_r exceeds the shortest relaxation time τ_1).

Note that $\lambda_{\mu r} \to 1$ for $\Delta t_r/\tau_\mu \to 0$, $\lambda_{\mu r} \to 0$ for $\Delta t_r/\tau_\mu \to \infty$, and always $0 < \lambda_{\mu r} < 1$. Denoting by p the value of μ for which $\tau_p < \Delta t_r < \tau_{p-1}$, one may put $\lambda_{\mu r} = 0$ for $\mu = 1, 2, \ldots, (p - 1)$, pro-

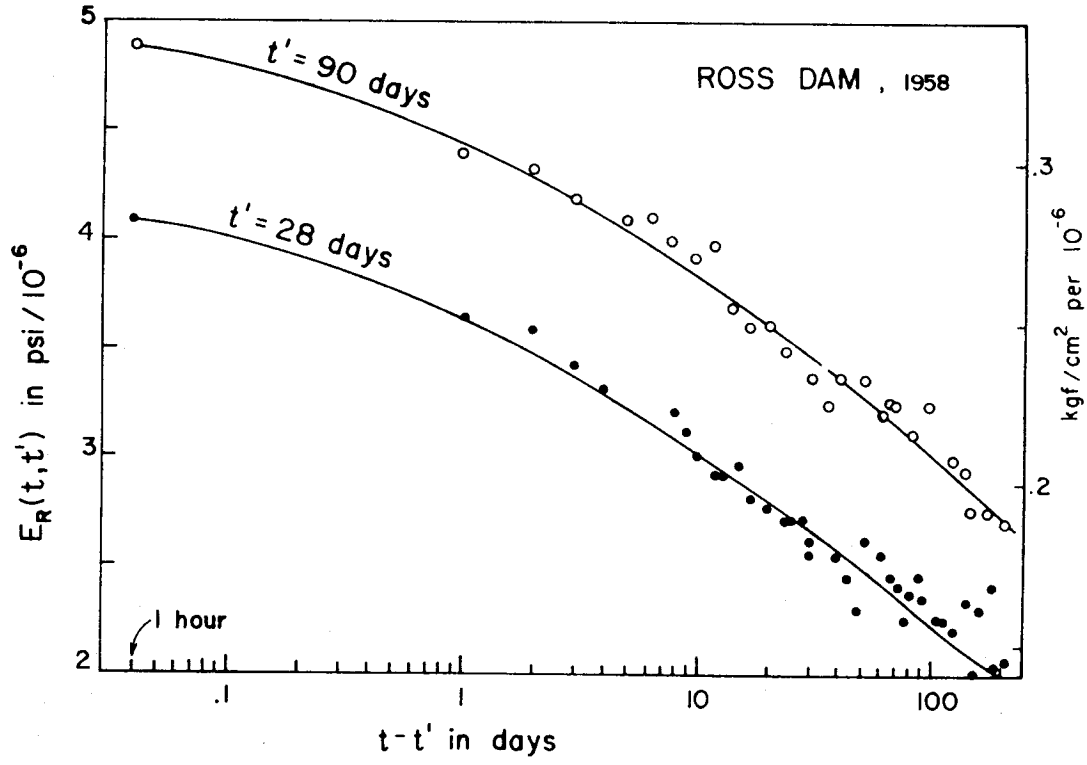
ROSS DAM , 1958
t' = 90 days
t' = 28 days
1 hour
$E_R(t,t')$ in psi / 10^{-6}
kgf / cm^2 per 10^{-6}
t - t' in days
5
4
3
2
.3
.2
.1
1
10
100

Fig. 10.

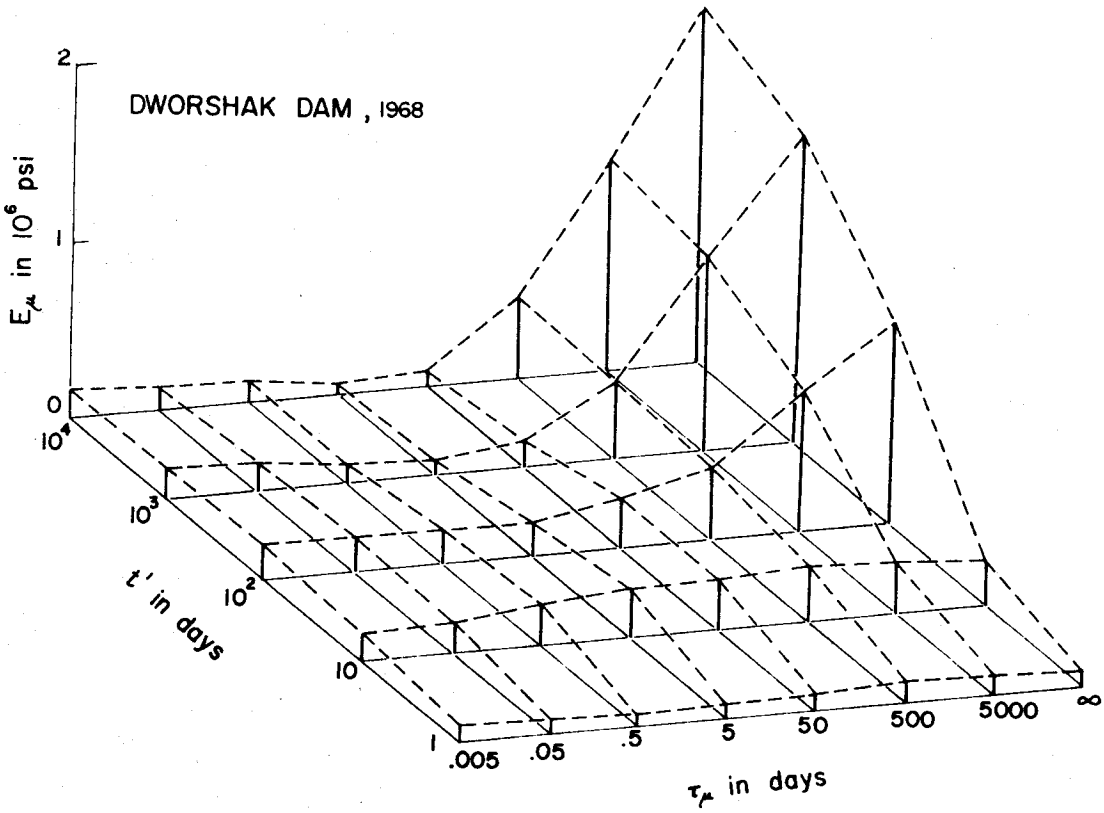
DWORSHAK DAM , 1968
E_μ in 10^6 psi
t' in days
τ_μ in days
2
1
0
10^4
10^3
10^2
10
1
.005
.05
.5
5
50
500
5000
∞

Fig. 11.

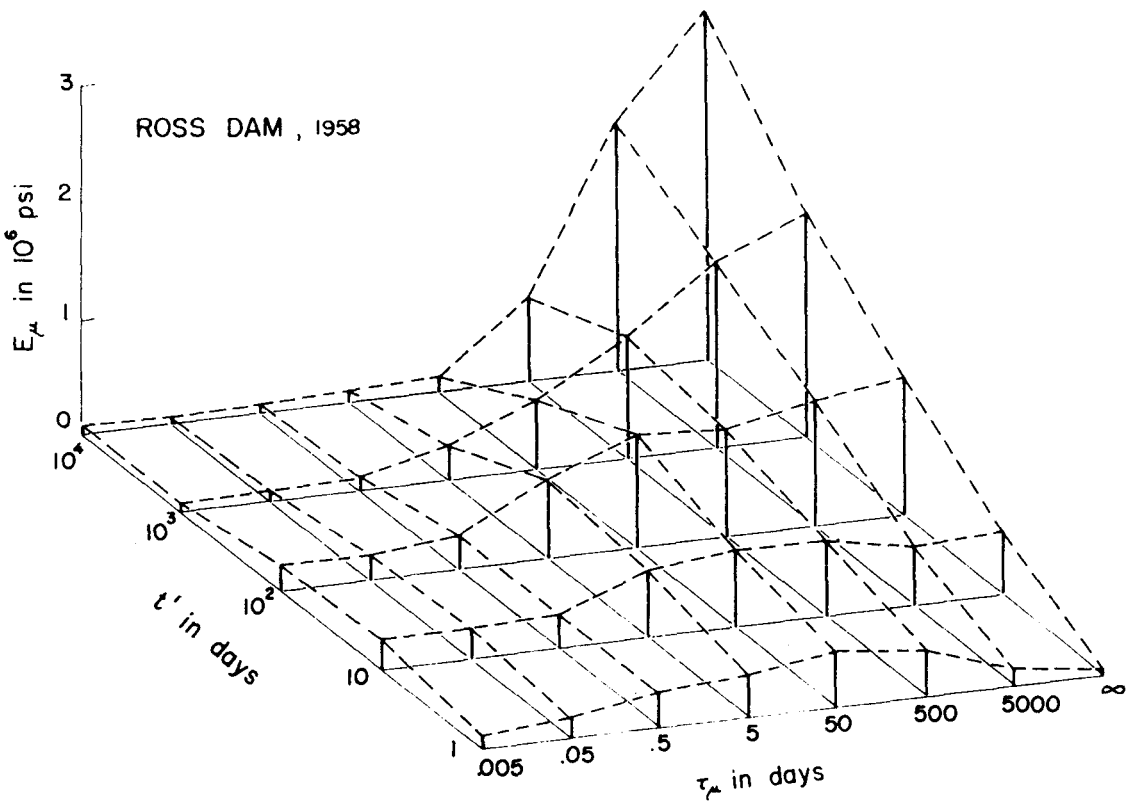
ROSS DAM , 1958
E_μ in 10^6 psi
3
2
1
0
10^4
10^3
10^2
10
1
t' in days
.005
.05
.5
5
50
500
5000
∞
τ_μ in days

Fig. 12.

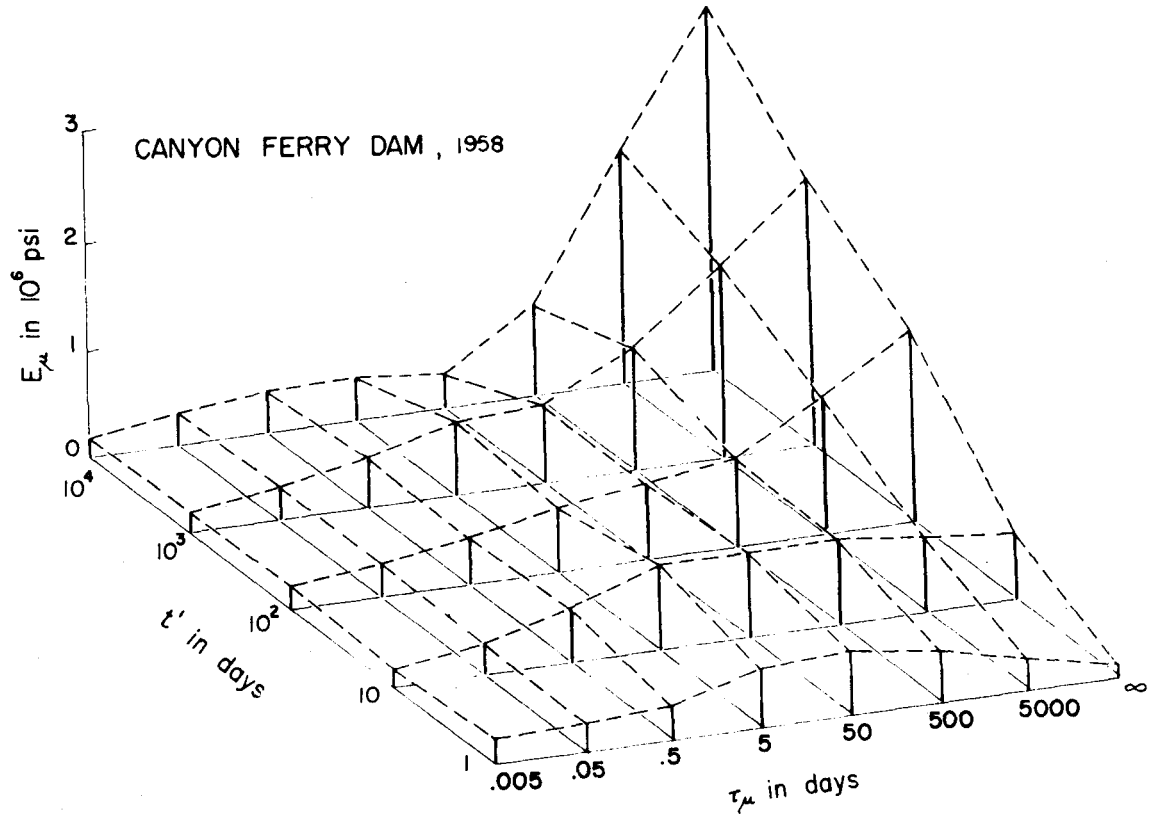
CANYON FERRY DAM , 1958
E_μ in 10^6 psi
3
2
1
0
10^4
10^3
10^2
10
1
t' in days
.005
.05
.5
5
50
500
5000
∞
τ_μ in days

Fig. 13.

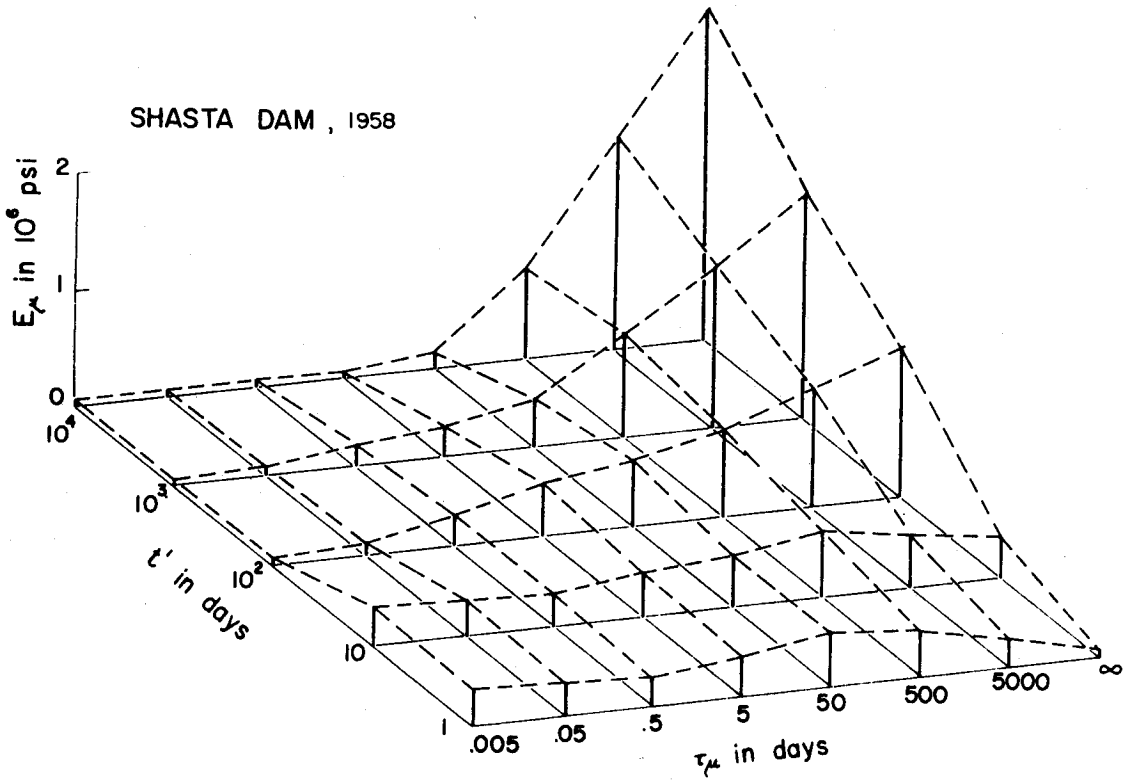
SHASTA DAM , 1958
$E_{\tau\mu}$ in 10^6 psi
2
1
0
10^4
10^3
10^2
10
1
t' in days
.005
.05
.5
5
50
500
5000
∞
τ_μ in days

Fig. 14.

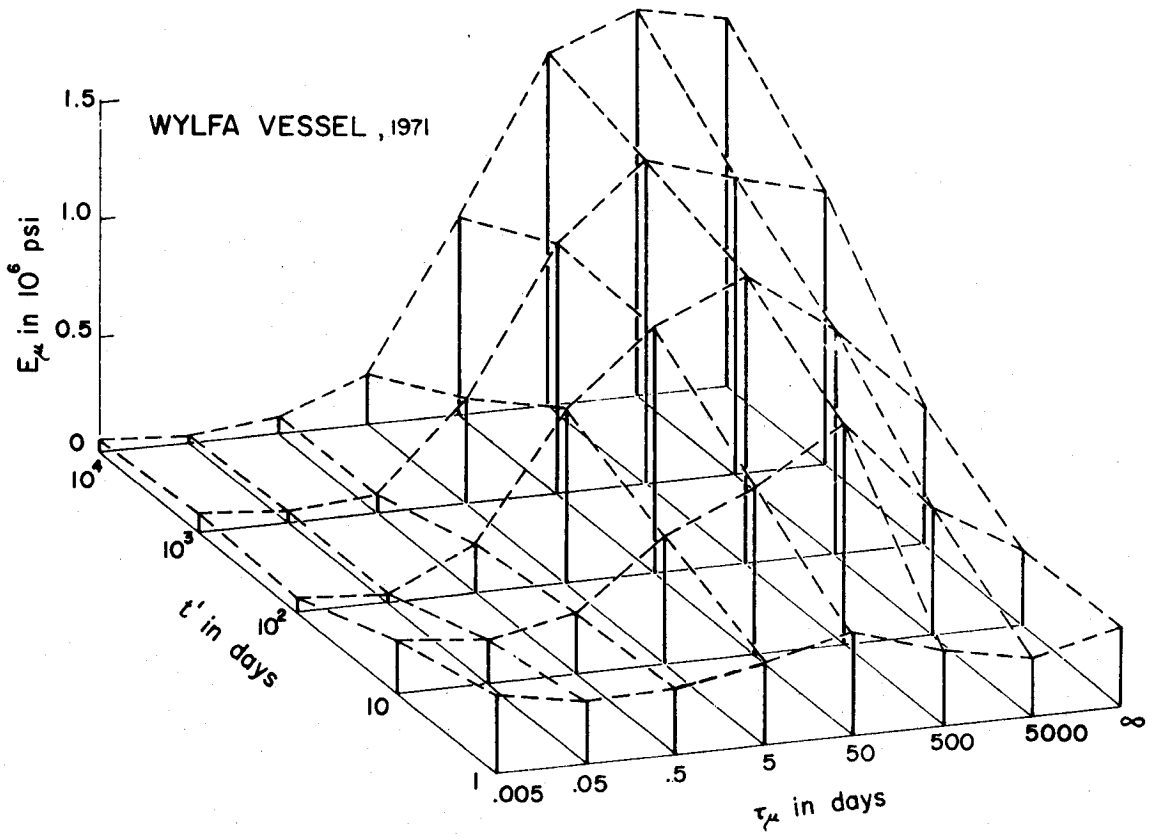
WYLFA VESSEL , 1971
$E_{\tau\mu}$ in 10^6 psi
1.5
1.0
0.5
0
10^4
10^3
10^2
10
1
t' in days
.005
.05
.5
5
50
500
5000
∞
τ_μ in days

Fig. 15.

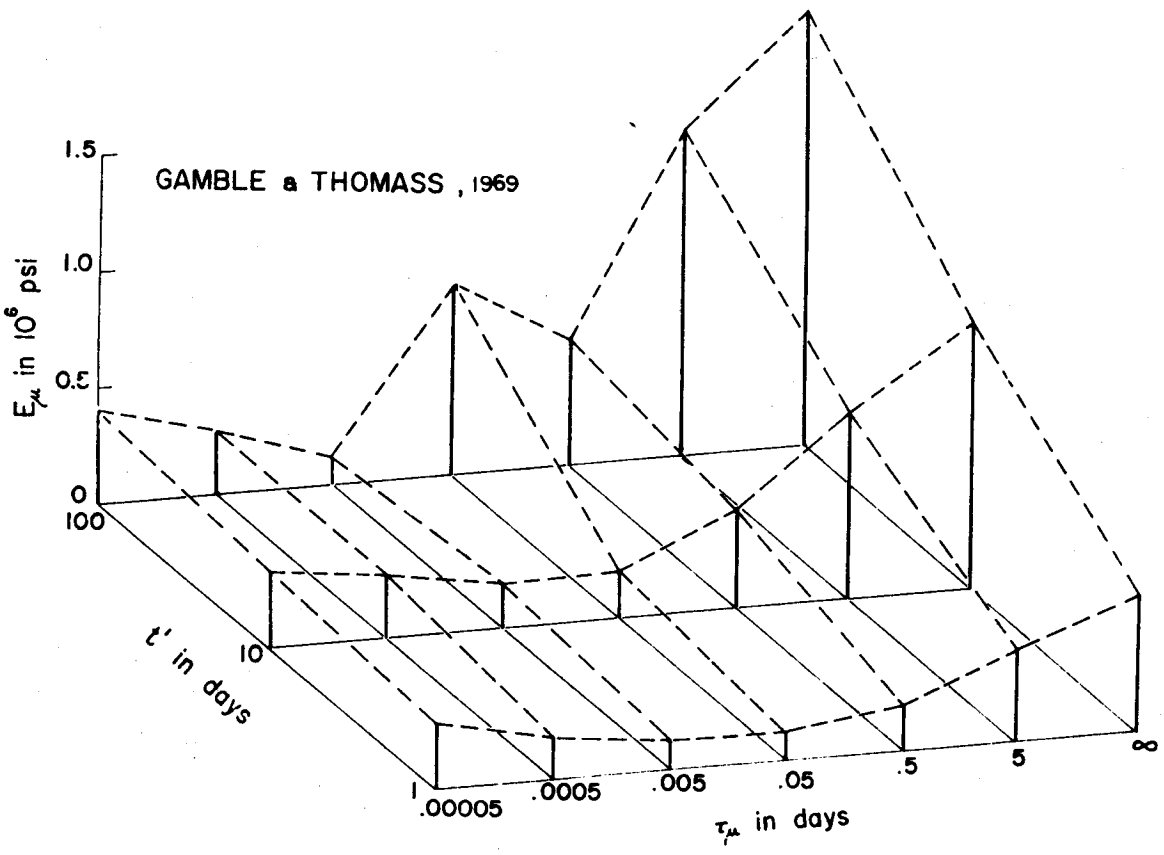
GAMBLE & THOMASS , 1969
E_μ in 10^6 psi
1.5
1.0
0.5
0
100
10
1
t' in days
.00005
.0005
.005
.05
.5
5
∞
τ_μ in days

Fig. 16.

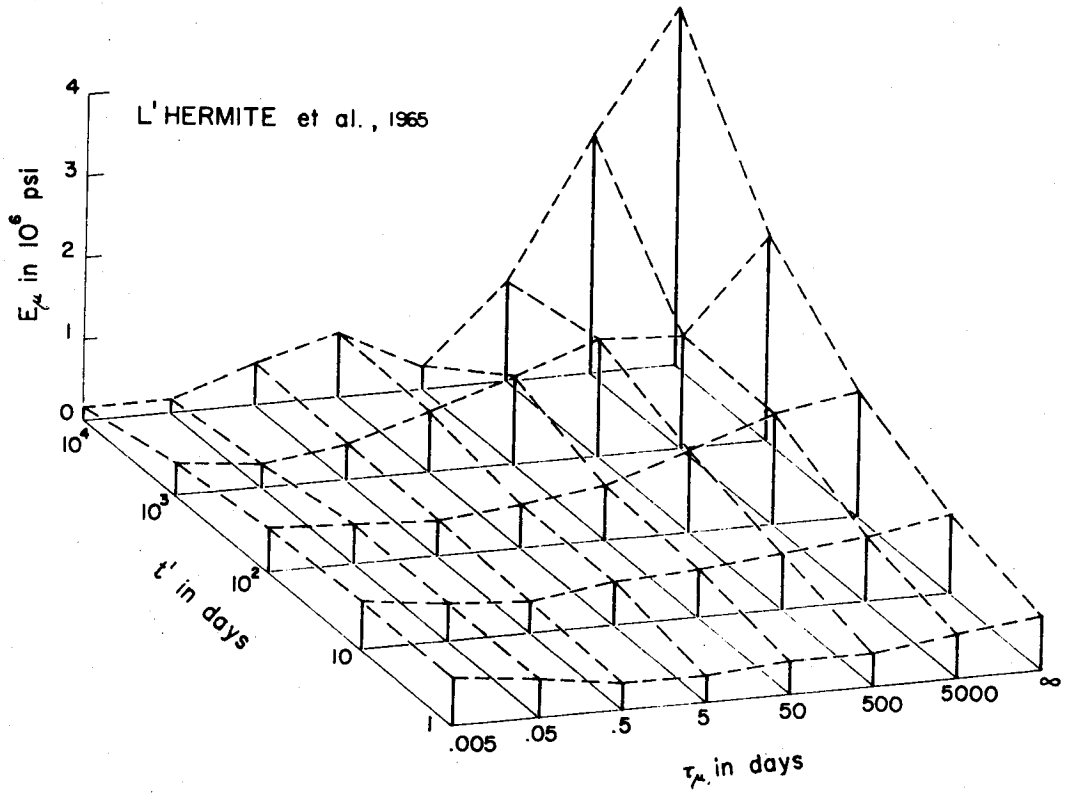
L'HERMITE et al., 1965
E_μ in 10^6 psi
4
3
2
1
0
10^4
10^3
10^2
10
1
t' in days
.005
.05
.5
5
50
500
5000
∞
τ_μ in days

Fig. 17.

TABLE II

Data	τ_μ	$10^4 E_{0_\mu}$	$10^4 E_{1_\mu}$	$10^4 E_{2_\mu}$	$10^4 E_{3_\mu}$	$10^4 E_{4_\mu}$	t'	w_1	w_2
Figs. 2, 9, 19 Ref. [14] Eq. (10)	.005	5.77	17.9	- 6.97	.811	0	1	.1	.1
	.05	2.33	23.0	- 9.66	1.18	0	10	.1	.1
	.5	- 1.38	34.3	- 16.0	2.06	0	100	.1	.1
	5.	- 2.60	46.9	- 24.2	3.23	0	1000	.1	.1
	50.	.755	48.9	- 25.8	3.49	0	10000	.1	.1
	500.	6.16	31.9	- 8.86	.869	0			
	5000.	11.2	-31.9	27.0	- 4.80	0			
	∞	15.2	-37.8	62.6	-10.4	0			
Figs. 3, 10 Ref. [15] [16] Eq. (11)	.005	-115.	196.	- 72.9	2.29	0	1	.5	0
	.05	- 81.6	147.	- 55.6	1.79	0	10	.2	0
	.5	- 76.0	153.	- 59.1	1.90	0	100	.2	0
	5.	-152.	291.	-106.	3.01	0	1000	.2	0
	50.	-143.	273.	- 86.2	1.53	0	10000	.2	0
	500.	-102.	170.	- 33.2	- .272	0			
	5000.	-105.	112.	7.21	- 1.05	0			
	∞	-112.	85.4	28.1	- 1.36	0			
Fig. 4 Ref. [15] [17] [16] Eq. (11)	.005	21.3	.650	- 1.61	.123	0	1	.1	.1
	.05	- 4.76	39.8	- 14.2	.486	0	10	.1	.1
	.5	- 31.4	93.0	- 31.1	.873	0	100	.1	.1
	5.	- 25.8	109.	- 34.4	.647	0	1000	.1	.1
	50.	12.8	59.4	- 13.3	- .389	0	10000	.1	.1
	500.	- 17.3	75.8	- 6.94	- .705	0			
	5000.	-138.	188.	- 25.7	.041	0			
	∞	-265.	314.	- 48.9	.980	0			
Fig. 5 Ref. [15] [16] Eq. (11)	.005	77.5	-38.6	- 1.90	.670	0	1	.5	0
	.05	39.0	1.75	- 10.8	.664	0	10	.2	.2
	.5	- 15.7	69.3	- 28.4	.827	0	100	.2	.2
	5.	- 30.6	96.6	- 33.7	.633	0	1000	.2	.2
	50.	10.1	50.1	- 14.3	- .113	0	10000	.2	.2
	500.	- 11.9	56.5	- 4.22	- .479	0			
	5000.	-102.	121.	- 4.27	- .582	0			
	∞	-132.	110.	21.4	- 1.49	0			
Fig. 6 Ref. [18] Eq. (11)	.005	69.4	0	- 36.7	6.57	-.353	1	.1	0
	.05	52.6	0	- 28.1	4.90	-.259	10	.1	0
	.5	23.1	0	4.82	- 2.22	.150	100	.1	0
	5.	- 17.7	0	66.2	-14.4	.816	1000	.1	0
	50.	- 28.1	0	85.5	-15.2	.783	10000	.1	0
	500.	- 47.0	0	92.8	-14.7	.742			
	5000.	- 30.3	0	59.3	- 7.50	.351			
	∞	47.0	0	- 25.8	10.9	.727			
Fig. 7 Ref. [19] Eq. (11)	.00005	- 29.3	77.4	- 22.5	0	0	1	.1	0
	.0005	- 31.4	72.6	- 21.9	0	0	10	.1	0
	.005	- 63.0	119.	- 43.1	0	0	100	.3	0
	.05	-120.	207.	- 75.8	0	0			
	.5	-103.	167.	- 44.2	0	0			
	5.	-103.	153.	- 8.90	0	0			
	∞	-109.	156.	8.56	0	0			
Fig. 8 Ref. [20] Eq. (11)	.005	56.2	0	11.7	- 4.21	.266	1	.1	0
	.05	34.7	0	16.0	- 4.61	.285	10	.1	0
	.5	22.4	0	17.0	- 3.85	.243	100	.1	0
	5.	29.7	0	9.29	- .141	-.024	1000	.1	0
	50.	33.1	0	5.91	3.78	-.441	10000	.1	0
	500.	11.1	0	32.4	- .309	-.236			
	5000.	2.59	0	55.8	- 4.38	-.170			
	∞	.783	0	67.1	- 6.26	.393			

τ_μ, t' are in days; E_μ in Eqs. (10), (11) is in psi.

vided that $\tau_\mu = 10^{\mu-1}\tau_0$. Then, according to (18) and (19),

$$E''_r = \sum_{\mu=p}^{m} \lambda_{\mu r} E_{\mu r-\frac{1}{2}} + E_{\infty r-\frac{1}{2}} \qquad (20)$$

$$E''_r \Delta\varepsilon''_r = \sum_{\mu=1}^{p-1} \sigma_{\mu r-1} + \sum_{\mu=p}^{m} \{ 1 - e^{-\Delta t_r/\tau_\mu} \} \sigma_{\mu r-1} + E''_r \Delta\varepsilon^0_r \qquad (21)$$

(As a crude approximation, one may further put $e^{-\Delta t_r/\tau_\mu} \approx 0$ and $\lambda_{\mu r} \approx 1$ for $\mu > p + 1$.) It is seen that those Maxwell units in the chain in figure 1 whose relaxation times τ_μ are substantially less than Δt_r pose no appreciable resistance to the deformation and drop out of action. This, of course, may also be expected on the basis of an intuitive judgment.

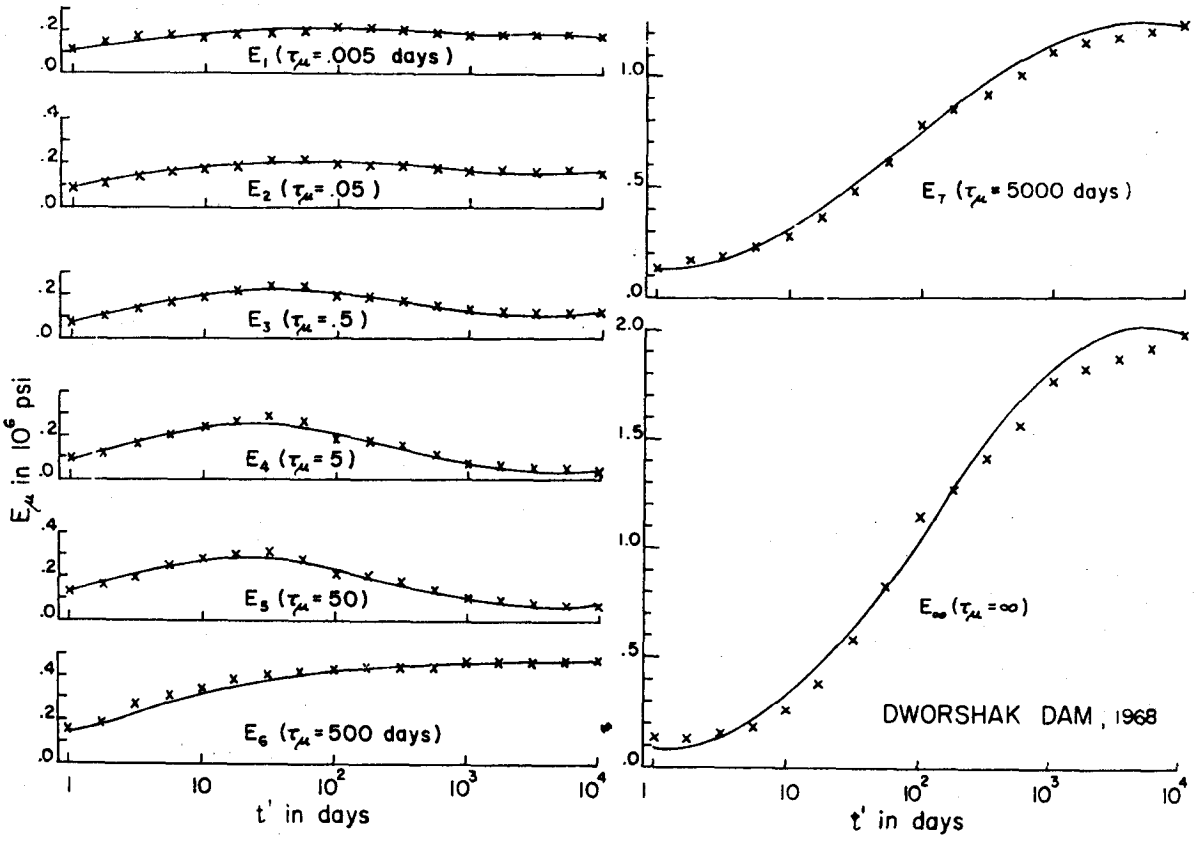

Fig. 18.

The algorithm presented above is analogous to the algorithm for the Kelvin chain model with time-dependent properties, published in Ref. [4] (Eq. 70-79). A similar algorithm for Kelvin chains which has been developed earlier by Zienkiewicz *et al.* [27] does not apply for concrete because the relation considered for springs ($\sigma_\mu = E_\mu \varepsilon_\mu$) is thermodynamically unacceptable when E_μ increases with age. Another similar algorithm for Maxwell chains, applicable to the special case of time-invariable viscoelastic materials and thermorheologically simple materials, has been presented by Taylor *et al.* [25].

ORGANIZATION OF THE PROGRAM FOR MAXWELL CHAIN IDENTIFICATION FROM GIVEN DATA

1. Values of $J(t, t')$ for selected values of t and t' are read. (If the given creep data do not cover the whole desired time range in both t and t-t', intuitive graphical extrapolation from given data must be done beforehand.)

2. Calling the interpolation subroutine for $J(t, t')$ values, the stress relaxation curves are computed from Eq. (12) for selected t'-values such as $t' = 1$, 10, 100, 1,000, 10,000 days (as in fig. 9 below). In the rare cases that the relaxation curves for the same specimens are available for some t'-values, the relaxation curves for these t'-values are also computed from the creep data and a weighted average of both curves is then taken.

3. Each relaxation curve is expanded in Dirichlet series (6), calling the least-square subroutine based on Eq. (8).

4. Moduli E_μ as functions of t' are smoothed by expression (10) or (9), calling another least square subroutine.

5. Stress relaxation curves are evaluated from $E_\mu(t')$ and plotted on Calcomp plotter to be compared visually with the relaxation data (if available).

6. Creep curves are computed from $E_\mu(t')$, using Eq. (17) with $\Delta\sigma_r = 0$ and Eq. (15). Then they are plotted on Calcomp plotter and compared visually with the given creep data.

If the fits of the given creep data, as well as of the relaxation data, are unsatisfactory, the program is run again for a different extrapolation of creep data and for different weights w_1, w_2, w_3 in Eq. (8). After some experience, however, repeated runs have usually been unnecessary.

NUMERICAL RESULTS AND FITS OF THE BEST AVAILABLE DATA

All of the extensive data that could be found in the literature on concrete at constant temperature and nearly constant water content [9 - 11 - 13 - 18 - 19 - 21]

were analyzed (using computer CDC-6400) with the above program (written in FORTRAN IV). The data points are shown in figures 2-8 and 10, and further information on the data used (including the references) is compiled in Table I. The solid lines in figures 2-8 represent the fits by Maxwell chain model, computed from E_μ as defined in Table II. Figure 10 shows the fit of the relaxation data measured on the same specimens as the creep data from figure 3. (The fit in figure 10 may be regarded as a confirmation of the superposition principle because the creep function was characterized almost uniquely by the creep data in figure 3.) For other data, relaxation measurements are not available. As is seen, all of the fits are quite satisfactory.

Most of the data had to be plotted in the $\log(t - t')$ — scale because the actual time scale obscures the misfit for all but one order of magnitude of time. (Unfortunately many hypotheses have been supported in the literature by fits in the actual time scale. Seemingly good fits are then easily obtained. But this practice is misleading and usually in the logarithmic time scale such fits would appear as unacceptable.) Whenever possible, the replotting of data points from the original papers was done with the help of a table of values [4, 24, 8].

Whereas all data points represent test results, the data in figure 6, as an exception, represent the design curves recommended for prestressed concrete reactor vessels.

In figures 3-8, the values of the instantaneous elastic modulus had to be judiciously estimated, for lack of information. The relaxation data in figure 10 were originally presented as the ratio $\sigma(t)/\sigma(t_0)$ where $\sigma(t_0)$ was the stress a short delay $t_0 - t'$ after time t' of strain enforcement; $\sigma(t_0)$ was 400 psi (for both t' shown) but the time lag $t_0 - t'$ was not reported. It was assumed as one hour, and, taking the E-modulus for one hour lag, E_R-values were computed from the original data points and plotted in figure 9. (If this assumption were inaccurate, the data points in figure 9 would all be shifted equal distance up or down).

The values obtained for the spring moduli E_μ of the Maxwell chain model (before smoothing by expressions (10) or (9)) are plotted in figures 11-17 against τ_μ and $\log t'$. Each series of E_μ-values for a fixed t' corresponds to what is called relaxation spectrum in classical viscoelasticity. The diagrams in figures 11-17 thus represent the relaxation spectrum as a function of age at loading, t'. Note that the surfaces formed by the relaxation spectra have similar forms for different concretes.

Figure 18 is an example of the fit by expression (10) (solid lines) with the E_μ-values from Table II. To check the quality of fit in detail, the relaxation curves have been computed in this case for four uniformly spaced t'-values per decade, as is seen from figure 18. Such dense point values of E_μ were necessary to decide which of expressions (10), (9), or (11) was the best one. Without using the smoothing term with w_1 and w_2 in Eq. (18), the sequence of data points would scatter much more than in figure 18.

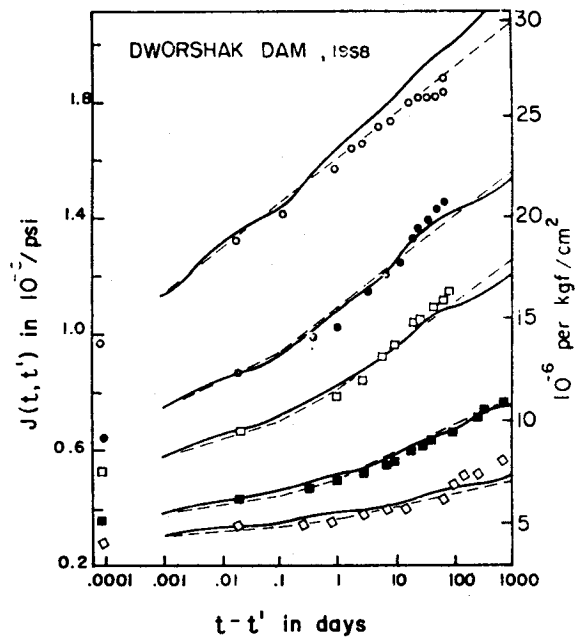

Fig. 19.

Function $J(t, t')$, representing the unit creep curves for various t' in figure 2-8, was computed from the expression for $E_\mu(t')$ given in Table I by means of the algorithm defined by Eq. (15)-(19). Four equal steps per decade in the logarithmic time scale were used. It is noted that the fits shown by solid lines in figures 2-8 could have been even closer to the original data points if the various smoothing operations had not been applied. The smoothing is inevitable, however, due to the high scatter of all data with regard to t'. (This scatter can be best demonstrated in plots of ε versus t' at constant t.)

The solid lines in figure 19 show how the same data as in figure 2 are fitted when more sparsely spaced τ_μ-s are chosen, namely $\tau_\mu = 0.005 \times 50^{\mu-1}$. As compared with the experimental error, the fit is still acceptable, though " bumpy ".

A crucial assumption in the present analysis is the principle of superposition, which is applicable when (*a*) the stress is less than about 0.5 of strength, so that no significant microcracking occurs, and (*b*) the water content is constant [3, 5]. The principal experimental data in its support, are, in addition to those in figure 10, the data of Ross [23]. In figure 20 they are replotted in log-time scale. Based on the smoothing of creep data by dashed-lines shown in figure 20, the stress relaxation curve given by a solid line was computed on the basis of the superposition principle. In spite of the fact that specimens in these tests were mildly drying (at 91 % relative humidity), the relaxation data conform well with the principle of superposition, in fact even better than Ross found originally [23] without the smoothing in log-time and by computations which in 1958 could not have been made accurately because electronic computers were unavailable. (Fig. 20 also shows the approximate predictions by the effective modulus method and the rate-of-creep method, as given in Ref. [23].

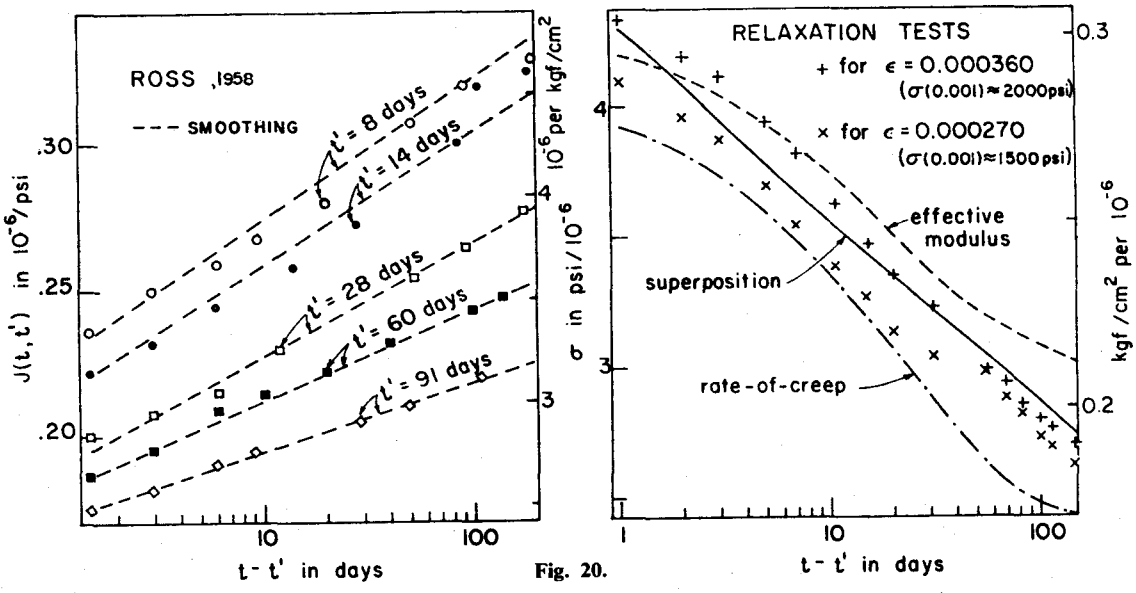

Fig. 20.

CONCLUSIONS

1. The linear creep behavior of concrete as an aging linearly viscoelastic material can be approximated, with any desired accuracy, by the Maxwell chain model (fig. 1) with age-dependent properties.

2. This model permits close and smoothed fits of test data, as figures 2-8 demonstrate.

3. The Maxwell chain representation can be obtained by expanding the relaxation function in Dirichlet series with age-dependent coefficients (Eq. 6), which is best accomplished by the method of least squares with a penalty term on first to third differences of coefficients as a smoothing devise (Eq. 8). The relaxation function needed may be computed from the creep data. The program outlined identifies the material parameters from any given test data very economically (in less than 15 sec. CPU time on CDC-6400).

4. Since conclusion 1 has previously been made [3] also for the Kelvin chain, both types of chains are mutually equivalent even for aging materials. But the Maxwell chain is more convenient for identification of material parameters from test data. (Both types of chains are also equivalent to any other possible model.)

5. The Maxwell chain representation proposed guarantees positiveness of all spring moduli E_μ and dashpot viscosities η_μ (if scatter of the data is not excessive). This permits giving the individual units of the chain a physical interpretation, associating them with various diffusion processes in the microstructure (see [4]), and opens the way toward rational generalizations to variable temperature [7, 3] and water content [5, 3].

6. For the Maxwell chain representation a new algorithm for creep structural analysis is presented (Eq. 15-19). It permits an arbitrary increase of the time step and uses only a few internal state variables (hidden stresses) for characterization of the whole history of the material. The resulting substantial reduction of machine time and storage requirements is valuable in the case of large finite element systems.

ACKNOWLEDGMENT

The present results have been achieved under the U.S. National Foundation Grant GK-26030. The authors wish to thank Mr. M. Mamillan, C.E.B.T.P., Paris, for providing a numerical table of the creep data in figure 8.

RÉSUMÉ

Une loi de fluage de type différentiel d'après une chaîne de Maxwell et relative au béton en cours de vieillissement. — *On montre que la loi de fluage linéaire du béton peut être caractérisée, avec toute la précision voulue, par une loi de fluage de type différentiel qu'on peut interpréter par un modèle de Maxwell en chaîne combinant les viscosités en fonction du temps et des modules de ressort. On identifie ces paramètres d'après les résultats d'essai en développant en séries de Dirichlet les courbes de relaxation qui sont elles-mêmes calculées d'après les courbes de fluage expérimentales. L'identification ne comporte qu'une seule solution si une certaine condition de régularisation est imposée aux spectres de relaxation. La formulation est importante lorsqu'on procède à une intégration graduelle dans le temps de systèmes à éléments finis plus grands, car ainsi il n'est pas besoin de stocker les données de l'évolution des contraintes. A cette fin, on propose un nouveau algorithme numérique inconditionnellement stable, qui permet un accroissement arbitraire de l'intervalle de temps à mesure que la vitesse de fluage décroît. La formulation de type différentiel permet d'établir une corrélation avec les processus de mouvement au niveau de la microstructure, et mène ainsi vers des généralisations rationnelles à températures et teneurs en eau variables. La chaîne de type Kelvin précédemment étudiée permet elle aussi une telle corrélation, mais l'identification des résultats d'essai est alors compliquée.*

REFERENCES

[1] BAŽANT Z.P. — *Numerical determination of long-range stress history from strain history in concrete.* Materials and Strcutures (RILEM), Vol. 5, 135-141, 1972.

[2] BAŽANT Z.P. — *Prediction of creep effects using the age-adjusted effective modulus method.* J. Amer. Concrete Inst., Vol. 69, 212-217, April 1972.

[3] BAŽANT Z.P. — *Theory of creep and shrinkage in concrete structure : A précis of recent developments.* Mechanics Today, Vol. 2, Pergamon Press (in press).

[4] BAŽANT Z.P. — *Thermodynamics of interacting continua with surfaces and creep analysis of concrete structures.* Nuclear Engineering and Design, Vol. 20, 477-505, 1972.

[5] BAŽANT Z.P., WU S.T. — *Creep and shrinkage law for concrete at variable humidity.* J. Eng. Mech. Div. Am. Soc. of Civil Engrs. (under review).

[6] BAŽANT Z.P., WU S.T. — *Dirichlet series creep function for aging concrete.* Proc. ASCE, J. Eng. Mech. Div., Vol. 99, EM2, Apr. 1973, 367-387.

[7] BAŽANT Z.P., WU S.T. — *Thermoviscoelasticity of aging concrete*, sent to Proc. ASCE, J. Eng. Mech. Div.; and Preprint No. 2110, ASCE Annual Meeting, New York, Oct.-Nov. 1973.

[8] BÉRÈS L. — *La macrostructure et le comportement du béton sous l'effet de sollicitations de longue durée.* Materials and Structures (RILEM), Vol. 2, p. 103-110, 1969.

[9] BROWNE R.D., BURROW R.E.D. — *An example of the utilization of the complex multiphase material behavior in engineering design.* Int. Conf. on " Structure, Solid Mechanics and Engineering Design in Civil Engineering ", p. 1343-1378, Editor M. Te'eni, J. Wiley - Interscience, 1971 (Univ. of Southampton, April 1969).

[10] GAMBLE B.R., THOMAS L.H. — *The creep of maturing concrete subjected to time varying stress.* Proceedings of the 2nd Australasian Conf. on the Mechanics of Structures and Materials, Adelaïde, Australia, Aug., 1969, Paper 24.

[11] HANSON J.A. — *A 10-year study of creep properties of concrete.* Concrete Laboratory Report No. Sp-38, U.S. Department of the Interior, Bureau of Reclamation, Denver, Colorado, July, 1953.

[12] HANSEN T.C. — *Estimating stress relaxation from creep data.* Materials Research and Standards (ASTM), Vol. 4, 1964, 12-14.

[13] HARBOE E.M. *et al.* — *A comparison of the instantaneous and the sustained modulus of elasticity of concrete.* Concrete Laboratory Report No. C-854, Division of Engineering Laboratories, U.S. Department of the Interior, Bureau of Reclamation, Denver, Colorado, March, 1958.

[14] HARDY G.M., RIESZ M. — *The general theory of Dirichlet series*, (Cambridge Tracts in Math. & Math. Phys. No. 18), Cambridge Univ. Press, 1915.

[15] KENNEDY T.W., PERRY E.S. — *An experimental approach to the study of the creep behavior of plain concrete subjected to triaxial stresses and elevated temperatures.* Res. Report 2864-1, Dept. of Civil Engineering, Univ. of Texas, Austin, 1970.

[16] KLUG P., WITTMANN F. — *The correlation between creep deformation and stress relaxation in concrete.* Materials and Structures (RILEM), Vol. 3, 75-80, 1970.

[17] LANCZOS C. — *Applied Analysis*, Prentice Hall, 1964 (p. 272-280).

[18] L'HERMITE R., MACMILLAN M., LEFÈVRE C. — *Nouveaux résultats de recherches sur la déformation et la rupture du béton.* Annales de l'Institut Technique du Bâtiment et des Travaux Publics, Vol. 18, No. 207-208, p. 325-360, 1965.

[19] NEVILLE A.M. — *Creep of concrete : plain, reinforced, prestressed*, North Holland Publ. Co., Amsterdam, 1970.

[20] NEVILLE A.M. — *Properties of concrete.* J. Wiley, New York, 1963.

[21] PIRTZ D. — *Creep characteristics of mass concrete for Dworshak Dam.* Report No. 65-2, Structural Engineering Laboratory, Univ. of California, Berkeley, California, Oct. 1968.

[22] ROSCOE R. — *Mechanical models for the representation of viscoelastic properties.* British J. of Applied, Physics, Vol. 1, 1950, 171-173.

[23] ROSS A.D. — *Creep of concrete under variable stress.* Amer. Concrete Inst. Journal, Proc. Vol. 54, 739-758, 1958.

[24] ROSTÁSY F.S., TEICHEN K.T., ENGELKE H. *Beitrag zur Klärung des Zusammenhanges von Kriechen und Relaxation bei Normalbeton.* Bericht, Otto-Graf-Institut, Universität Stuttgart, Strassenbau und Strassenverkehrstechnik, Helf 139, 1972.

[25] TAYLOR, R.L., PISTER K.S., GOUDREAU G.L. *Thermomechanical analysis of viscoelastic solids.* Intern. J. for Numerical Methods in Engineering, Vol. 2, 45-60, 1970.

[26] WITTMAN F. *Über den Zusammenhang von Kriechverformung und Spannungsrelaxation des betons.* Beton- und Stahlbetonbau, Vol. 66, p. 63-65.

[27] ZIENKIEWICZ O.C., WATSON M., KING I.P. — *A numerical method of viscoelastic stress analysis.* Intern. J. Mech. Sciences, Vol., 10, 807-827, 1968.